

Single-Grasp, Model-Free Object Classification using a Hyper-Adaptive Hand, Google Soli, and Tactile Sensors

Zak Flintoff, Bruno Johnston, and Minas Liarokapis

Abstract — Robots need to use their end-effectors not only to grasp and manipulate objects but also to understand the environment surrounding them. Object identification is of paramount importance in robotics applications, as it facilitates autonomous object handling, sorting, and quality inspection. In this paper, we present a new hyper-adaptive robot hand that is capable of discriminating between different everyday objects, as well as ‘model’ objects with the same external geometry but varying material, density, or volume, with a single grasp. This work leverages all the benefits of simple, adaptive grasping mechanisms (robustness, simplicity, low weight, adaptability), a Random Forests classifier, tactile modules based on barometric sensors, and radar technology offered by the Google Soli sensor. Unlike prior work, the method does not rely on object exploration, object release or re-grasping and works for a wide variety of everyday objects. The feature space used consists of the Google Soli readings, the motor positions and the contact forces measured at different time instances of the grasping process. The whole approach is model-free and the hand is controlled in an open-loop fashion, achieving stable grasps with minimal complexity. The efficiency of the designs, sensors, and methods has been experimentally validated with experimental paradigms involving model and everyday objects.

I. INTRODUCTION

Object identification and the extraction of object properties using vision or force / tactile sensors has become extremely important for a variety of human robot interaction applications. Nowadays, robots have started operating in human-centric, dynamic and unstructured environments and they are used to execute increasingly dexterous tasks. For robots to be able to effectively interact with their surroundings they need first to identify the objects or the tools that they will use. This is one of the most challenging problems in robotics and although several vision-based classification approaches have been proposed, in everyday environments, poor lighting conditions, occlusions, or camera limitations may restrict their application. A feasible alternative that can overcome these limitations is to perform object classification using force or tactile sensing. Methodologies using such sensors can even derive specific object properties including size, texture, stiffness, shape, and weight [1]–[4] or to distinguish between different objects using various classifiers [5]–[7].

*Both B. Johnston and Z. Flintoff are considered first authors.
B. Johnston, Z. Flintoff, and M. Liarokapis are with the New Dexterity research group, Department of Mechanical Engineering, Faculty of Engineering, The University of Auckland, 20 Symonds St, Auckland 1010, New Zealand. Email: minas.liarokapis@auckland.ac.nz

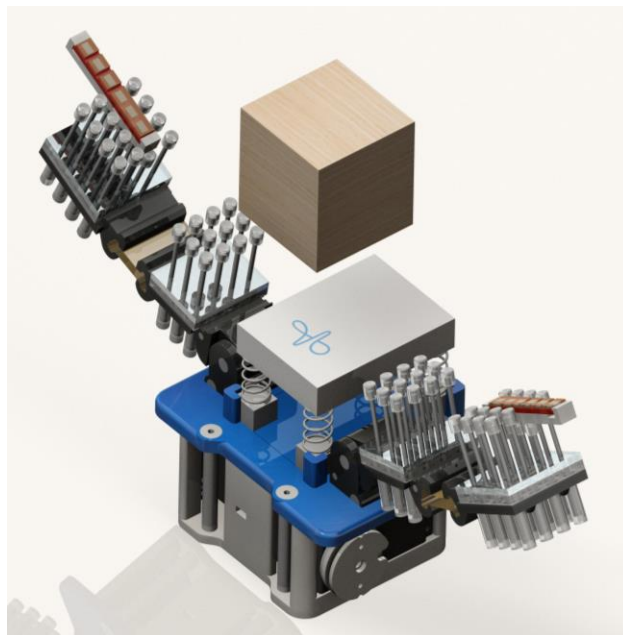


Fig. 1. A 3D model of an adaptive, compliant and underactuated robot hand equipped with hyper-adaptive finger-pads, tactile sensors and the Google Soli radar sensor. The robot hand was developed by the New Dexterity research group (www.newdexterity.org).

Furthermore, both manipulation and grasp stability can be optimized when object properties are taken into consideration during the planning process (e.g., through minimization of the contact forces necessary to achieve stable grasps). Identification of object class also enables the execution of object-specific strategies or plans [8]. Specific object properties such as shape and size can influence grasp configuration, while weight, friction, and stiffness can affect the external contact forces that are acting on the object and which are required to ensure grasp stability.

In this paper, we present a new hyper-adaptive, underactuated, compliant robot hand (please see Fig. 1) equipped with force sensors and a Google Project Soli sensor, that can discriminate between different everyday objects with a single grasp. The work done in this paper improves upon and extends the work done in [9] and [10] and has two key objectives. The first objective is to present a new hyper-adaptive, underactuated, compliant robot hand that provides improved grasp stability over the underactuated hands employed in [9] and [10]. Please note that the term “hyper-adaptive” is used here to denote a highly adaptive mechanism that efficiently conforms to different object geometries. Each hyper-adaptive finger has one pin and one flexure joint and is

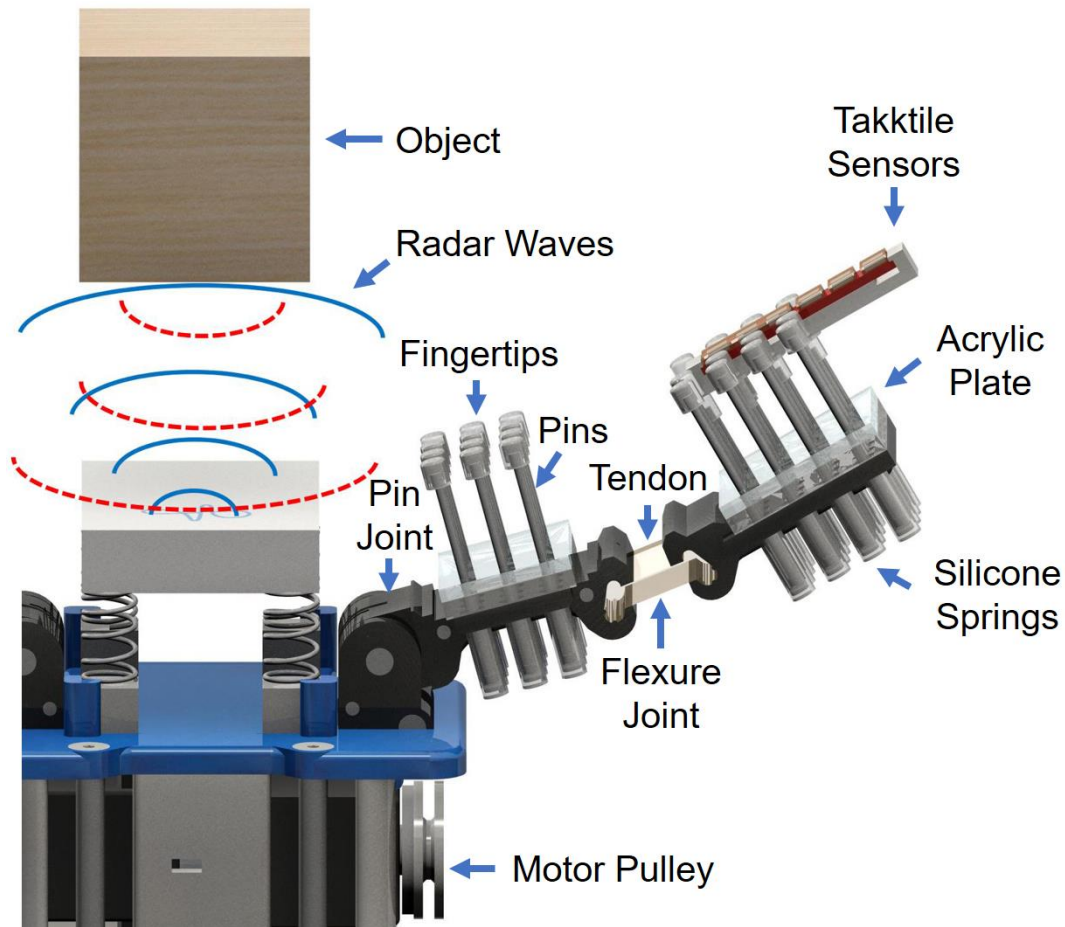


Fig. 2. Close-up view of the structure of a finger of the hyper-adaptive robot hand. The hand design is symmetric. Each robot finger has two phalanges with hyper-adaptive finger-pads, one spring loaded pin joint and one flexure joint based on elastomer material (Smooth-On PMC 780 urethane rubber).

equipped with hyper-adaptive finger-pads and 6 pressure sensors (please see Fig. 2). These design features allow for simple open-loop control of the robot hand, meaning the classification process and results are not affected by the controller parameters. Accurate grasp planning is thus not required, and the system is model-free.

The second objective is to extend the methods used in [9] and [10] to classify common objects, by adding a Google Soli sensor to differentiate between ‘model’ objects having identical external geometries but differing in material, density, or volume. This objective has been achieved by applying the Random Forests (RF) classification algorithm to features extracted from the raw tactile sensors data and the Google Soli sensor data, recorded during grasping. Using the RF inherent feature variables importance calculation procedure, the most important features are also derived. Such information can lead to optimized robot hand designs as well as to improved object classification algorithms. The efficiency of the proposed methods is experimentally validated using both everyday life and ‘model’ objects. As the object classification system presented in this paper is both rapid and reliable, we propose that the system is well suited for use in demanding robotics applications, such as object sorting and quality inspection.

The rest of the paper is organized as follows: Section II discusses the related work, Section III presents the designs, the sensors, and the methods used in this work, Section IV presents the experiments conducted, Section V reports and discusses the results, while Section VI concludes the paper and discusses future directions.

II. RELATED WORK

In recent years, the field of tactile based object classification has benefited from advances in sensor technology. Due to the complexity of analyzing tactile sensor data, the methods presented in the literature mainly employ data driven approaches. Sophisticated control methods and exploratory procedures are also necessitated by some of these methods. Object properties such as rigidity, material and texture of the object are used for deciding the object class.

In [11], three rigidity levels of the objects were determined using piezo-resistive pressure sensors. A Decision Tree classifier was employed, with the mean, the variance and the maximum force values used as features. The material of the objects was identified by sliding the finger on the object surface in [12] while using a 6-axis force/torque sensor attached to the fingertip.

Data from a multimodal sensor that provides force, vibration and temperature data was used in [13] for texture recognition. Data from this sensor was collected by sliding the finger on the object surface with a predefined trajectory. In [14], the authors used robotic exploratory procedures and 34 adjectives to describe the objects, as absorbent, compact, cool, metallic, unpleasant etc. Additionally, pressure, temperature, and deformation information of the contact surfaces were provided by the biomimetic sensor.

The popular vision-based object recognition technique ‘bag-of-features’ was adapted to identify the object class with tactile sensing in [15]. A ‘vocabulary’ of tactile images was formed using this method, by grasping a set of objects with varied poses. This method generates histograms for each class in the training set and during identification it compares them against a new histogram generated from grasping observations collected online. In [16], a k-Nearest Neighbors classifier was applied to the time series of tactile-array images during squeezing and de-squeezing (releasing) of the object to achieve object classification. The grip on the object was however lost during identification due to the need to collect data for the de-squeezing phase. By using a single, stable grasp in our case, we do not require a de-squeezing motion, so the grasp can be maintained during and after classification. Mobility and rigidity information of the object together with its class is identified by the method used in [17]. This paper also involves a k-Nearest Neighbors classifier being applied to data collected from sliding a tactile array on the object surface.

Raw sensor data is used for tactile based object identification, performed by reinforcement learning techniques in both [7] and [17]. In [18], a 1-vs-all classifier is obtained by using time series of sensor measurements and Spatio-Temporal Hierarchical Matching Pursuit (STHMP), performed on raw data to build feature hierarchies for 10 household objects. Joint position information was used in conjunction with tactile data in [7] to increase success rates. An incremental learning technique facilitates an online improvement of the employed classifier. A multimodal tactile sensor is integrated into a Shadow dexterous robot hand in [19] which provides force, vibration, and temperature data. Rigidity, texture and thermal properties of the object are extracted in this study through a series of exploratory movements. Data is again processed using reinforcement learning techniques. Multimodal object recognition was recently achieved in [20], using a four fingered hand and by employing Deep Learning methods. Force sensor arrays, 6 axis force/torque sensors for each fingertip, and joint encoders were used to collect the required data and the impact of each sensor on the recognition performance was assessed.

Similar work to ours is detailed in [21]. A single grasp was used for classification as in our work. This method also forms a feature vector with data collected upon events (when first contact of the fingers is detected, and in steady state) as opposed to those works that use time series data. A capacitive

sensor was attached to the gripper of a PR2 robot during the experiments. Fullness of the containers is recognized in these experiments and all the objects used in the experiments have radial symmetry, therefore the results do not confirm that the approach is robust to variance in object orientation. The hybrid control scheme which switches between velocity and force control in this method differentiates from ours as our scheme utilizes simple, open-loop control. Open-loop control is an advantage of our work, as complicated controller design was required in [21], due to the effect of controller parameters on the classification performance. In [9] and [10], we presented similar work using a simple, adaptive robot hand that was equipped with simple tactile sensors and a Random Forests classifier, achieving a classification accuracy of 94% for a set of everyday life objects and 93% to 94% for various model objects with different stiffness, sizes, and shapes. The proposed method could not however discriminate between different object materials, as no Google Soli was available, and a simpler adaptive robot hand was used. Finally, the work in [22] has inspired our approach to using Google Soli as it proposes a radar system for material and object classification.

III. DESIGNS, SENSORS & METHODS

A. A Two-Fingered Hyper-Adaptive Robot Hand

The hyper-adaptive robot hand described in Fig. 1 uses a base and a palm module developed by the New Dexterity research group, utilizing two Dynamixel MX-64AR motors. The base has an appropriate compliant support for the positioning of the Google Soli sensor that allows it to conform to the object geometry during the post-contact, hand-object system reconfiguration. The fingers were based on the fingers of the Yale Open Hand Model T42 [23] and were modified to include hyper-adaptive finger-pads. Each finger uses a spring loaded pin joint at the base and a flexure joint between the two phalanges.

The hyper-adaptive finger-pads consist of simple, easy to manufacture parts, using silicones (Smooth-On Ecoflex 00-30) and steel pins. The array of pins fits inside a deformable silicone mold that allows the pins to conform to the object geometry as contact is made and force is applied. The compliance of these finger-pads allows the fingers to reconfigure to the object shape, distributing the contact forces and ensuring the stability and robustness of the grasp. The pins are placed within holes machined into an acrylic plate and have a tight tolerance to ensure they are constrained to through-plane motion. Silicone pads are fitted to the contact tips of the pins to provide a high friction surface for contact. The distal finger pad has a 4x4 array of pins, while the proximal has a 4x3 array. More details can be found in Fig. 2, where a close-up view of the finger structure is presented. The robot hand developed is symmetric and both fingers have the same geometry. The robot hand weighs 830 g (with the Google Soli and the tactile sensors attached) and it has an angular aperture of 140 degrees and an aperture of 260 mm. Regarding the force exertion capabilities, each

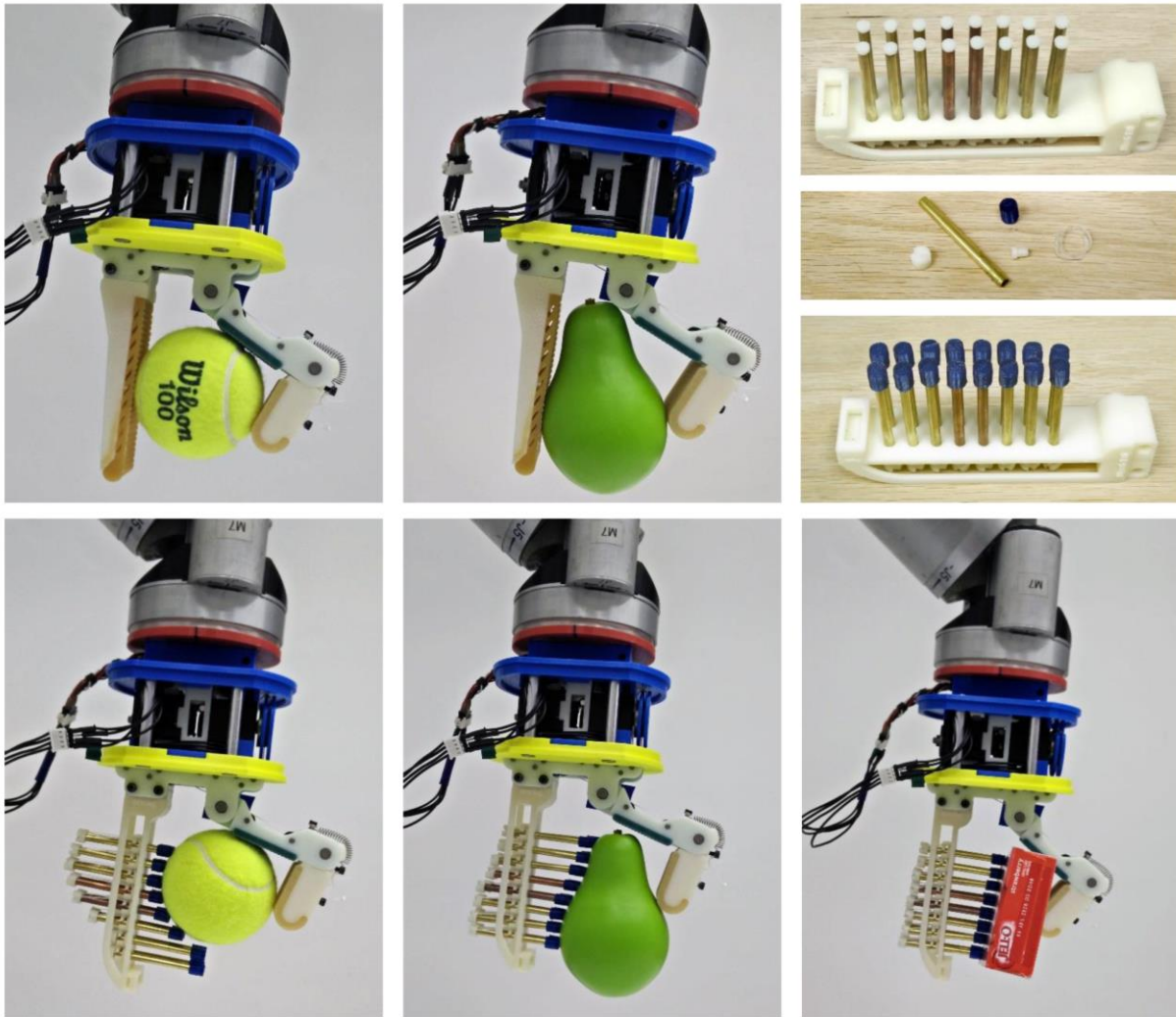


Fig. 3. Another example of a hyper-adaptive robot gripper with a hyper-adaptive ‘thumb’ and an adaptive finger with two phalanges and two spring loaded pin joints. The hyper-adaptive gripper is compared with a simple gripper with a fixed thumb (row 1). The grasps involve a tennis ball (column 1), a plastic pear (column 2), and a paper box (column 3). The parts of the hyper-adaptive finger-pad are depicted in the top right sequence of images.

pin of the hyper-adaptive finger-pad can exert 1.2 N before being fully compressed. The maximum force that can be exerted per finger with fully compressed pins, is 60 N.

The design of the hyper-adaptive finger-pads can be easily incorporated to other robot hand designs, if there is enough space on the finger geometry to accommodate the required pins. An alternative implementation of the hyper-adaptive finger-pads concept can be found in the robot gripper that is presented in Fig. 3. This robot gripper has a steady thumb that accommodates a hyper-adaptive finger-pad and the under-actuated and compliant robot finger of the Yale Open Hand Model T42 [23].

B. Google Soli Sensor

The Google Project Soli sensor is a radar-based sensor that emits millimeter-scale wavelength radio frequency signals. The direction of the electromagnetic radio frequency waves is controlled by the antenna beam pattern and the energy of the radio frequency waves is either absorbed or scattered by objects obstructing the propagation path. Super-

imposed reflected signals are received by the transducer, and appropriate software is used to locate and describe the dynamics and the properties of the scattering centers. The Google Soli sensor has been proven in [22] to be useful for material identification. The energy of reflected waves is however also affected by the object pose, with corner geometries, and flat surfaces perpendicular to the transmitted wave reflecting the most energy. The contribution of object pose to this phenomena has been mitigated in this work by using a mechanical design that reduces variation in the final pose of the objects within the hand. The Google Soli sensor is located above the hand palm and is supported by an elastic structure on the robot palm that has four corner springs, in order to ensure a better conformability to the object geometry during grasping and reconfiguration.

C. Tactile Sensors

For sensing contact and forces exerted on the grasped object, tactile sensors have been integrated into the hyper-adaptive finger-pads on the distal phalanges. The low-cost

Table I. Features used for classification

#	Feature	Description
1	Aperture	The sum of the motor positions when contact with the object is first detected for both fingers
2	First contact forces (Sum)	The sum of the contact forces for initial contact of both fingers
3	Final contact forces (Sum)	The sum of the final contact forces of both fingers at the completion of the grasp
4	Contact force gradient (Sum)	The sum of the gradients of the contact forces between first and final contact of both fingers
5	Final force (Sum)	The sum of all tactile sensor readings upon grasp completion
6	Soli Acceleration	Overall acceleration in the workspace of Soli
7	Soli Energy Total (Mean)	Total reflected energy
8	Soli Moving Energy (Mean)	Energy measured from the time-varying component of the reflected radar signal
9	Soli Strongest Energy Component (Mean)	Energy reflected from the most dominant target component
10	Soli Fine Displacement (Mean)	Related to the post contact fine displacement of the grasped object
11	Soli Fine Displacement (Time)	Related to the timing of the post contact fine displacement of the grasped object
12	Soli Fine Displacement (Polynomial Constants)	Related to the post contact fine displacement of the grasped object
15		
16	Soli Movement Index	The level of movement of the most dominant component
17	Soli Sonar (Mean)	Sonar value
18	Soli Spatial Dispersion (Mean)	The measure of the medium permittivity
19	Soli Velocity	Overall velocity of the object
20	Soli Velocity Centroid	Weighted average of the overall velocity

and reliable ‘Takktiler’ sensors are based on MEMS barometers mounted on printed circuit boards with a cast rubber coating to spread the load [24]. Each finger has 6 sensors, with all sensors located on the distal phalanx. The sensors interface via a ‘Takkfast’ data collection module to the control PC using a USB cable. The Takktiler sensors have excellent linearity (typically <1%) and low noise (<0.01 N), and the external addressing circuitry allows multiple sensors to communicate on the same bus at frequencies of more than 100 Hz.

D. Random Forests based Classification

The machine learning methodology presented in this paper is based on a Random Forests classifier. The classification models are used to discriminate between the different object classes and solve two different problems: 1) classification of material, density, or volume for cubes and cylinders, 2) classification of a range of everyday life

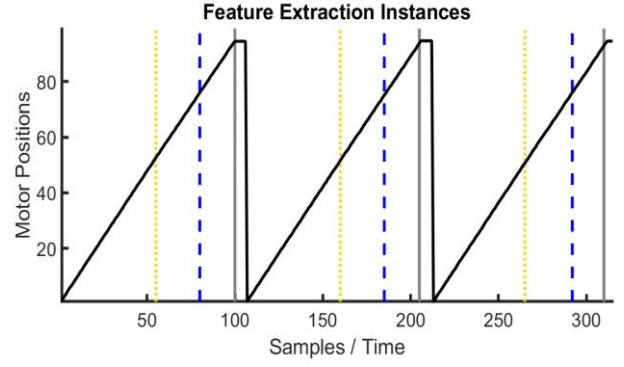


Fig. 4. Example of automatic contact detection and feature extraction. The back lines denote the motor positions, the dotted yellow lines denote the first contact with the left finger and the dashed blue lines the first contact with the right finger. The solid grey lines denote the end of the hand-object system reconfiguration (“completion” of the grasp). Data from a random, single experiment (3 repetitions), are presented.

objects. Random Forests was originally proposed by Tin Kam Ho of Bell Labs [25] and Leo Breiman [26] and is a popular ensemble classifier based on a combination of decision trees. This paper deals with a multiclass classification problem (identifying multiple everyday objects) and a multidimensional feature space, as the feature vector consists of 20 different feature variables. The choice of the classifier was based on the work done in [10], where Random Forests provided the best prediction accuracy out of a range of commonly used classifiers. Random Forests offer excellent predictive performance and a feature variables importance calculation procedure that can sort the features based on their importance.

E. Features Selection & Features Importance Calculation

The feature space used consists of the Google Soli readings, the motor positions and the contact forces exerted at different instances of the grasping process. We chose to use the readings at specific time instances instead of time series, in order to reduce the computational complexity of the classification. We have also verified that the use of time series does not offer any meaningful improvement of the predictive performance. Features related to the motor positions and the contact forces are extracted using an automated detection method (see Fig. 4). For a detailed description of all the feature variables that are used in this paper, please see Table I.

One of the main goals of this study is to identify the most important features for object classification / identification. This is particularly useful for us, as this is a topic of great interest for our research group and such knowledge may help us optimize our robot hand designs in order to select the appropriate locations for the tactile sensors or to optimize our object classification algorithms. To do so, we have used the Random Forests feature variables importance calculation procedure using the mean decrease in accuracy method. The values of the importance scores have been normalized to allow for more intuitive comparisons. Results are reported in subsection V-C.

Table II. Characteristics of the everyday life objects that were examined. The objects are sorted by size.

Objects	Dimensions (mm)	Material
Squash Ball	40.5 \emptyset	Rubber
Marble	45 \emptyset	Glass
Cylinder	50x50 \emptyset – 4mm Wall	ABS Plastic
Cylinder	50x50 \emptyset – 5mm Wall	PLA Plastic
Cylinder	50x50 \emptyset – 6mm Wall	ABS Plastic
Cylinder	50x50 \emptyset – 8mm Wall	ABS Plastic
Cylinder	50x50 \emptyset – 14mm Wall	ABS Plastic
Hollow Fill Cylinder	50x50 \emptyset	PLA Plastic
Solid Fill Cylinder	50x50 \emptyset	PLA Plastic
Cylinder	50x50 \emptyset	Mild Steel
Cylinder	50x50 \emptyset	Wood
Cube	50x50x50	PLA Plastic
Cube	50x50x50	Mild Steel
Cube	50x50x50	Wood
Cricket Ball	70 \emptyset	Plastic and Cork
Cylinder	50x70 \emptyset	PLA Plastic
Cube	70x70x50	PLA Plastic
Cardboard Box	31x112x146	Cardboard
Computer Mouse	35x60x110	Plastic
Cylinder	50x90 \emptyset	PLA Plastic
Empty Can	110x73 \emptyset	Tin (empty)
Full Can	110x73 \emptyset	Tin (corn inside)
Soft Drink Can	167x63 \emptyset	Aluminum
Glass Bottle	156x69 \emptyset	Glass
Syrup Bottle	65x90x180	Plastic
Spray Bottle	35x104x276	Plastic

IV. EXPERIMENTS

In this section, we present the selected objects and the experiments that we conducted in this study.

A. Selected Objects

In this work, we use a wide range of everyday life objects of different sizes, shapes, and stiffness, as well as model objects with controlled properties (objects of the same size and shape but of different material). The characteristics (size and material) of all objects used in this study are reported in Table II.

B. Experiments Conducted

The experimental setup involved positioning the hand on a table surface such that the grasping action of the hand was on the same plane. An arbitrary position on the table surface, within the hand workspace / grasp, was then assigned for each object. For every trial, the object was rested at the assigned location with a variation in the object’s position and orientation of ± 10 mm and ± 10 degrees respectively. The experimental procedure then involved closing the hand to grasp the object while data was recorded from the tactile

and Google Soli sensors. Upon contact with the object surface the robot fingers reconfigured towards an elastic equilibrium configuration that was determined by the contact forces exerted. This reconfiguration moved the grasped object towards the wrist where the Google Soli sensor was located. Once a stable grasp of the object was achieved, data recording was ended, and the object was released. The experiment was repeated with the same object for a total of 10 trials. This procedure was performed for all the objects presented in Table II.

V. RESULTS

In this section, we present the classification results for objects with controlled properties and everyday life objects, and a ranking of the most important features as determined by the Random Forests feature variables importance calculation procedure.

A. Grasping Experiments

A series of experiments were conducted to evaluate the efficiency of the hyper-adaptive finger-pads in extracting stable and robust grasps (please see Fig. 3 and 5). For most objects tested, the length of the pins enabled a better grasp as this allowed larger conformability to the object geometries. However, in our testing we did note that for very small objects (smaller than a squash ball) the pins of the proximal and distal phalanges could meet each other before encountering the object to be grasped. This did have an impact on the quality of the grasp as it affects how the fingers of the hand close on the object. Regarding the applicability of the particular design in different grasping scenarios, the pins could be easily used in other hand designs, especially in hands with relatively wide fingers (to enable the use of the silicone springs). It is important to note that the pins can be placed in any orientation and can be of any length, completely up to the discretion of the designer (please see Fig. 3). The length of the pins and the silicone springs will simply affect how much deformation they are capable of, with orientation determining in what direction the hyper-adaptive finger-pad is most conformable. A video containing some grasping experiments can be found at the following URL:

<http://www.newdexterity.org/hyperadaptive>

B. Classification Results

For the training of the classifiers, we use the simple, 10-fold cross-validation method, to assess how the classification results will generalize to an independent data set. The classification accuracies were averaged over the multiple rounds of the cross-validation method. The Random Forests were grown for 100 trees, since such a value gives a good classification accuracy without severely increasing the computational complexity (decision takes <10 ms). The prediction accuracy for all 26 objects in the object set was over 99%. This set included three cubes of the same size but of different material (wood, PLA, and metal), four hollow, ABS cylinders having the same outer radius and height but

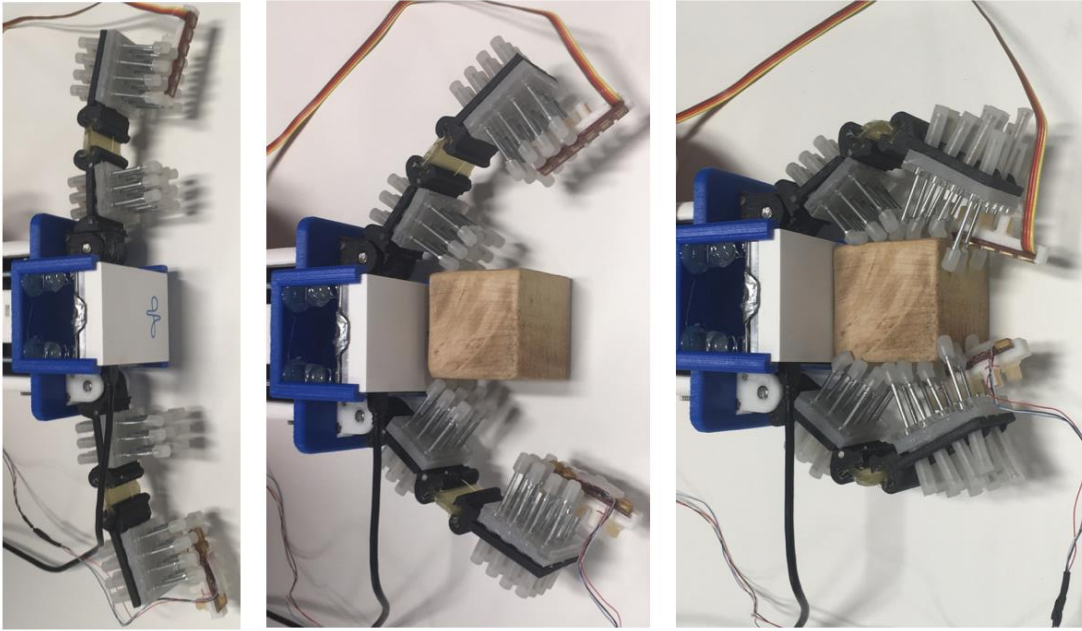


Fig. 5. Steps of the grasping and object identification processes. The system can identify the object using a single, open-loop, model-free grasp.

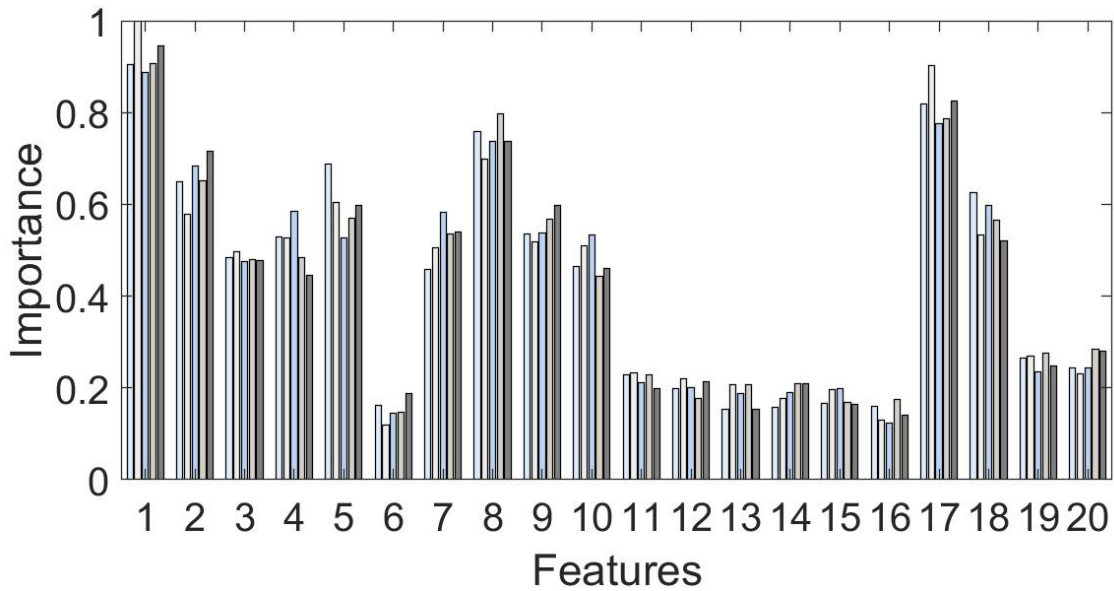


Fig. 6. Feature variables importance bar-plots. The height of the different bar-plots represents the importance scores of the different feature variables. The 20 features are described in Table I. The feature importance has been calculated for five different partitions of the training data and it is evident that the values are consistent across the five barplots of each feature.

different inner radius, two solid PLA cylinders having the same size but different fill densities, and other everyday life objects. It must also be noted that we conducted initial experiments that are not included in this study which reveal that the variations in the object pose do not appear to affect the overall classification performance.

C. Assessing the Feature Variables Importance

In this subsection, we calculate the feature variables importance using the inherent procedure of the Random Forests classifier and we assess the results. The importance bar-plots of the different feature variables for the problem of

discriminating between all the examined objects, are presented in Fig. 6. For each feature the importance scores have been calculated 5 times (for different partitions of the training data) and it can be observed that the importance values are consistent among partitions. It is also clear that specific features are more important than others. For example, features 1, 8, and 17, namely the motor aperture, Soli's moving energy, and Soli's sonar reading, have the highest feature importance scores across all features. On the other hand, features 6 and 16, Soli's acceleration and Soli's movement index, are of low importance, and thus are contributing less to the ability of the classifier to identify the

examined objects. This information could be utilized in future work for the optimization of the classifier (e.g., to use less feature variables without compromising the classification accuracy).

D. Limitations

Although the proposed hand design exhibits an improved grasping performance (grasp stability), it must be noted that it is not as efficient for small objects (as discussed in subsection V-A). Additionally, it cannot be used for the execution of dexterous manipulation tasks, as the hyper-adaptive finger-pads enclose the examined objects, constraining their motion within the hand. Moreover, the hand cannot be used in anthropomorphic designs due to space, packaging, and aesthetics constraints. It should also be noted that larger variations in the initial pose of an object may compromise the predictive performance and that new experiments are required to investigate this issue in detail.

VI. CONCLUSIONS AND FUTURE DIRECTIONS

In this paper, we proposed a hyper-adaptive robot hand design that combines the Google Soli radar sensor and tactile sensors to facilitate the execution of single-grasp, model-free object classification tasks. The hand conforms to the object geometry, offering increased robustness and stability in the execution of grasping tasks. A Random Forests classifier was used to discriminate between the examined objects, using the raw sensor values (no sensor calibration was required) and the motor positions in different time instances.

Regarding future directions, we plan to revisit the design of the hyper-adaptive robot hand, optimize the sensor selection and placement, assess the role of object pose variations and their effect on the identification accuracy, as well as develop new algorithms for haptic object classification that will account for highly unstructured environments.

REFERENCES

- [1] F. De Boissieu, C. Godin, B. Guilhamat, D. David, C. Serviere, and D. Baudois, "Tactile texture recognition with a 3-axial force MEMS integrated artificial finger.," in *Robotics: Science and Systems*, 2009, pp. 49–56.
- [2] T. Bhattacharjee, J. M. Rehg, and C. C. Kemp, "Inferring Object Properties from Incidental Contact with a Tactile Sensing Forearm," *ArXiv e-prints*, no. 1409.4972, Sep. 2014.
- [3] B. Frank, R. Schmedding, C. Stachniss, M. Teschner, and W. Burgard, "Learning the elasticity parameters of deformable objects with a manipulation robot," in *IEEE/RSJ International Conference on Intelligent Robots and Systems*, 2010, pp. 1877–1883.
- [4] J. Sinapov, V. Sukhoy, R. Sahai, and A. Stoytchev, "Vibrotactile Recognition and Categorization of Surfaces by a Humanoid Robot," *IEEE Trans. Robot.*, vol. 27, no. 3, pp. 488–497, Jun. 2011.
- [5] M. Schopfer, M. Pardowitz, R. Haschke, and H. Ritter, "Identifying Relevant Tactile Features for Object Identification," in *Towards Service Robots for Everyday Environments*, Springer, Berlin, Heidelberg, 2012, pp. 417–430.
- [6] A. Drimus, G. Kootstra, A. Bilberg, and D. Kragic, "Classification of rigid and deformable objects using a novel tactile sensor," in *15th International Conference on Advanced Robotics (ICAR)*, 2011, pp. 427–434.
- [7] H. Soh and Y. Demiris, "Incrementally learning objects by touch: online discriminative and generative models for tactile-based recognition.," *IEEE Trans. Haptics*, vol. 7, no. 4, pp. 512–25, Jan. 2014.
- [8] R. S. Johansson and J. R. Flanagan, "Coding and use of tactile signals from the fingertips in object manipulation tasks.," *Nat. Rev. Neurosci.*, vol. 10, no. 5, pp. 345–59, May 2009.
- [9] M. Liarokapis, B. Calli, A. Spiers, and A. Dollar, "Unplanned, Model-Free, Single Grasp Object Classification with Underactuated Hands and Force Sensors," *IEEE/RSJ Int. Conf. Intell. Robot. Syst.*, pp. 5073–5080, 2015.
- [10] A. J. Spiers, M. V Liarokapis, B. Calli, and A. M. Dollar, "Single-Grasp Object Classification and Feature Extraction with Simple Robot Hands and Tactile Sensors," *IEEE Trans. Haptics*, vol. 9, no. 2, pp. 207–220, Apr. 2016.
- [11] I. Bandyopadhyaya, D. Babu, A. Kumar, and J. Roychowdhury, "Tactile sensing based softness classification using machine learning," in *IEEE International Advance Computing Conference (IACC)*, 2014, pp. 1231–1236.
- [12] H. K. Lam *et al.*, "A study of neural-network-based classifiers for material classification," *Neurocomputing*, vol. 144, pp. 367–377, Nov. 2014.
- [13] J. A. Fishel and G. E. Loeb, "Bayesian exploration for intelligent identification of textures.," *Front. Neurobot.*, vol. 6, p. 4, Jan. 2012.
- [14] V. Chu *et al.*, "Using robotic exploratory procedures to learn the meaning of haptic adjectives," in *IEEE International Conference on Robotics and Automation*, 2013, pp. 3048–3055.
- [15] A. Schneider, J. Sturm, C. Stachniss, M. Reisert, H. Burkhardt, and W. Burgard, "Object identification with tactile sensors using bag-of-features," in *IEEE/RSJ International Conference on Intelligent Robots and Systems*, 2009, pp. 243–248.
- [16] A. Drimus, G. Kootstra, A. Bilberg, and D. Kragic, "Design of a flexible tactile sensor for classification of rigid and deformable objects," *Rob. Auton. Syst.*, vol. 62, no. 1, pp. 3–15, Jan. 2014.
- [17] T. Bhattacharjee, J. M. Rehg, and C. C. Kemp, "Haptic classification and recognition of objects using a tactile sensing forearm," in *IEEE/RSJ International Conference on Intelligent Robots and Systems*, 2012, pp. 4090–4097.
- [18] M. Madry, L. Bo, D. Kragic, and D. Fox, "ST-HMP: Unsupervised Spatio-Temporal feature learning for tactile data," in *IEEE International Conference on Robotics and Automation*, 2014, pp. 2262–2269.
- [19] D. Xu, G. E. Loeb, and J. A. Fishel, "Tactile identification of objects using Bayesian exploration," in *IEEE International Conference on Robotics and Automation*, 2013, pp. 3056–3061.
- [20] A. Schmitz, Y. Bansho, K. Noda, H. Iwata, T. Ogata, and S. Sugano, "Tactile object recognition using deep learning and dropout," in *14th IEEE-RAS International Conference on Humanoid Robots*, 2014, pp. 1044–1050.
- [21] S. Chitta, M. Piccoli, and J. Sturm, "Tactile object class and internal state recognition for mobile manipulation," in *IEEE International Conference on Robotics and Automation*, 2010, pp. 2342–2348.
- [22] H.-S. Yeo, G. Flamich, P. Schrempf, D. Harris-Birtill, and A. Quigley, "RadarCat: Radar Categorization for Input & Interaction," in *29th Annual Symposium on User Interface Software and Technology*, 2016, pp. 833–841.
- [23] R. Ma and A. Dollar, "Yale OpenHand Project: Optimizing Open-Source Hand Designs for Ease of Fabrication and Adoption," *IEEE Robot. Autom. Mag.*, vol. 24, no. 1, pp. 32–40, 2017.
- [24] L. P. Jentoft, Y. Tenzer, D. Vogt, R. J. Wood, and R. D. Howe, "Flexible, stretchable tactile arrays from MEMS barometers," *16th Int. Conf. Adv. Robot.*, pp. 1–6, 2013.
- [25] Tin Kam Ho, "Random decision forests," in *3rd International Conference on Document Analysis and Recognition*, 1995, vol. 1, pp. 278–282.
- [26] L. Breiman, "Random forests," *Mach. Learn.*, vol. 45, no. 1, pp. 5–32, 2001.